Surface area and pore size determination

24 November 2017

Annette Trunschke

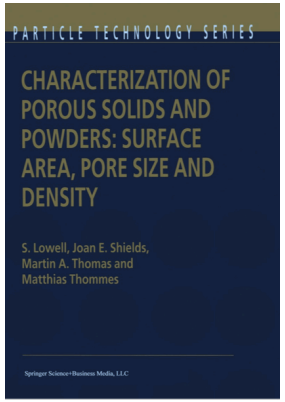

Further reading

S. Lowell, J.E. Shields, M.A. Thomas, M. Thommes, Characterization of Porous Solids and Powders: Surface Area, Pore Size and Density, Kluwer Academic Publisher, Dordrecht, 2004, Springer 2006.

R. Brdička, Grundlagen der physikalischen Chemie, Deutscher Verlag der Wissenschaften, Berlin 1982.
P.W. Atkins, J. de Paula, Physikalische Chemie, Wiley-VCH, Weinheim 2013.
G. Wedler, H.-J. Freund, Lehrbuch der Pysikalischen Chemie, Wiley-VCH, 2012.

F. Schüth, K.S.W. Sing, J. Weitkamp (Eds.), Handbook of Porous Solids, Vol. 1, Wiley-VCH, Weinheim 2002.

G. Ertl, H. Knözinger, J. Weitkamp (Eds.), Handbook of Heterogeneous Catalysis, VCH, Weinheim, 1997.

LECTURE SERIES
HETEROGENEOUS CATALYSIS

Heterogeneous catalysis

- Heterogeneous catalysis happens at the interface between phases
- The number of active sites depends on the surface area

- Surface area is related to
  - Particle size
  - Particle morphology
  - Surface texturing
  - Porosity

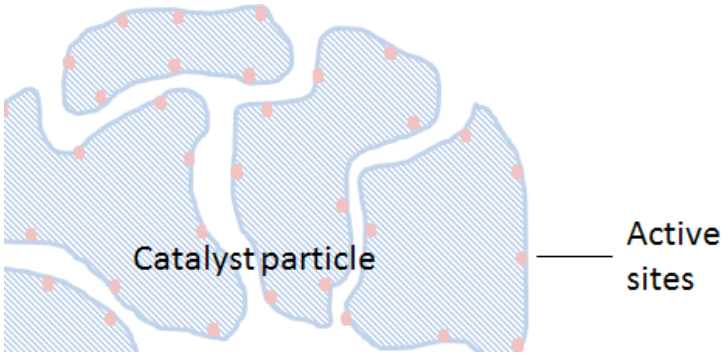

- The accessibility of active sites requires pores that allow molecular transport
- Porosity: fraction of the total void volume with respect to the volume of the catalyst
- Texture: - pore size
  - pore size distribution
  - pore shape

Heterogeneous catalysis

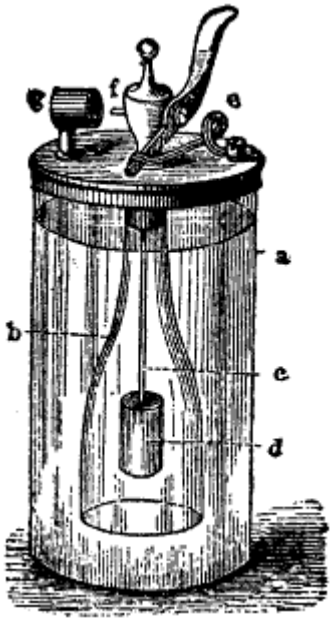

$$(NH_4)_2[PtCl_6] \xrightarrow{600\text{-}800^\circ C} \text{Pt with high surface area}$$

$$2\,H_2 + O_2 \rightarrow 2\,H_2O$$

Johann Wolfgang Döbereiner ‘s lighter (1823)

Some catalysts and support materials in heterogeneous catalysis

adsorbent	surface area [m^2/g]
charcoal	300 - 2500
silica gel	300 -350
γ-alumina	200 - 500
zeolites	500 - 1100

High surface area materials

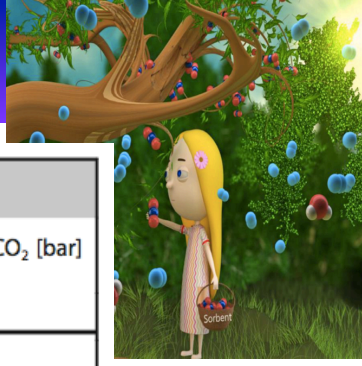

Table 2. List of leading CO_2 capture sorbents.

Supporting porous material	Amine type	CO_2 adsorption [mmol g^{-1}] Dry CO_2	Wet CO_2	Sorption temperature [°C] (adsorption–desorption)	Sorption partial pressure of CO_2 [bar] (adsorption–desorption)
MCM-41[11]	Polyethylenimine	2.02	2.98	75–75	0.15–0
SBA-15[12]	(3-Trimethoxysilylpropyl) diethylenetriamine	2.4	2.72	60–>300	0.15–0
Mesoporous silica capsules[13]	Tetraethylenepentamine	–	7.93	75–100	0.1–0
Mesoporous silica foam[14]	Tethered amines	–	11.8	25–100	0.08–0
Mg-MOF-74[15]	*N,N'*-Dimethyl ethylene diamine (mmen)	3.1	2.7	40–120	0.15–0
PPN-6-CH_2DETA[16]	Linear amines	3.04	–	22–80	0.15–vacuum
COP-19[17]	Polyethylenimine	1.57	2.27	40–80	0.15–vacuum
Hollow fibres (continuous)[18]	Amine impregnated silica	–	0.58	35–120	0.1–0
Aqueous amines[19]	Monoethanolamine (MEA)	–	0.83	80/120–120	0.15–0

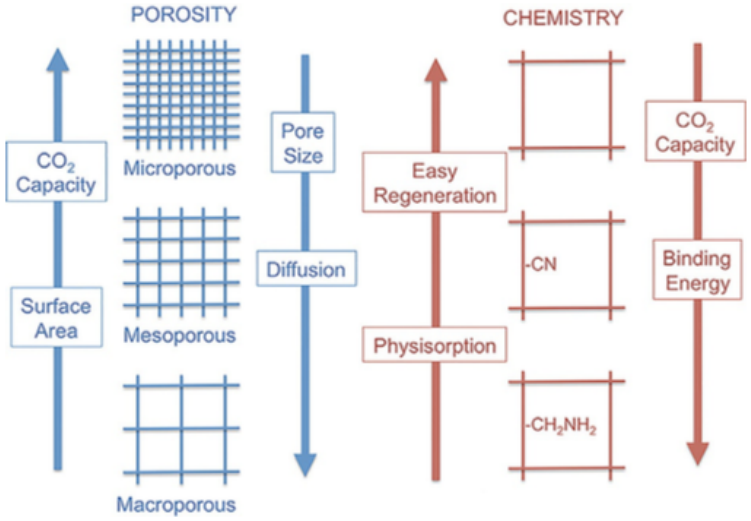

Dry condition (carbamate formation)

Primary amines

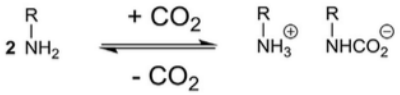

Humid condition (bicarbonate formation)

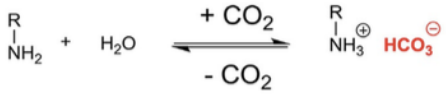

Table 3. Benchmark checkpoints for an effective CO_2 sorbent. All conditions have to be met to get the best working sorbent.

Checkpoint	Desired
Capacity	>2 mmol CO_2 per g of sorbent
Recyclability	>1000 cycles
Selectivity	>100 (CO_2/other gases)
Stability	>150 °C, boiling water, H_2S, SO_x, NO_x, HCl, NaOH, mechanical strength with low attrition index (AI)
Cost	<\$50 kg^{-1} (sorbent cost <\$10 kg^{-1})
Kinetics	>1 mmol $(g \times min)^{-1}$

ChemSusChem ***2017****, 10, 1303 – 1317.*

Factors affecting surface area

1 particle of edge lenght = 1 m

10^{18} particles of edge lenght = 10^{-6} m

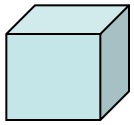

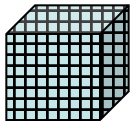

size

S=6 m^2

S_i=6x10^{-12} m^2 S_{total}=6x10^6 m^2

MgO

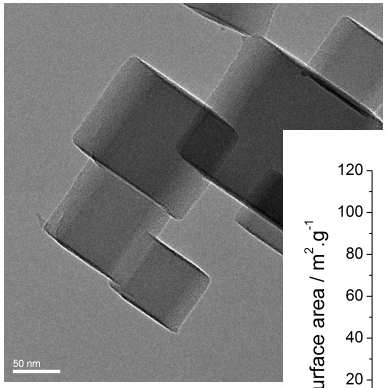

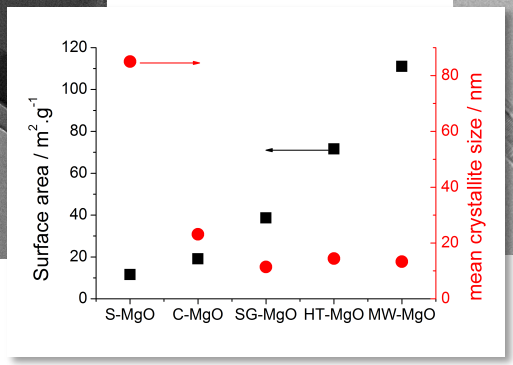

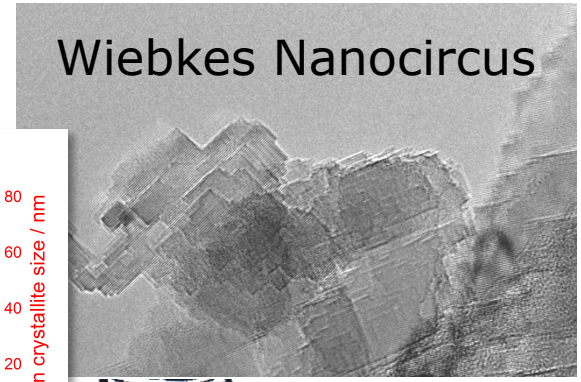

shape
roughness

S=10 m^2g^{-1}

S=100 m^2g^{-1}

Zeolite ZSM-5

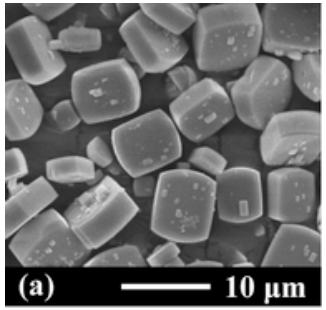

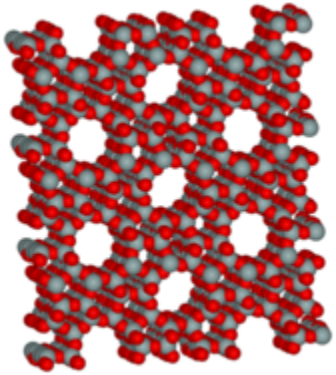

S=400 m^2g^{-1}

porosity

Catal. Sci. Technol., ***2014***, *4, 4265-4273.*

Surface area measurements

- Surface area from particle size distribution

  Dynamic light scattering

  Measures Brownian motion and relates this to the size of the particles by using a correlation function and the Stokes-Einstein equation

  Non-spherical particles will be measured as equivalent spheres

$$D_0 = \frac{kT}{6\pi\eta R}$$

D= Diffusion coefficient
k= Boltzmann constant
T= absolute temperature
η= dynamic viscosity of the solvent
R= radius of the particle

- Microscopy

  Shape analysis

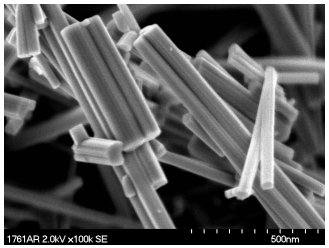

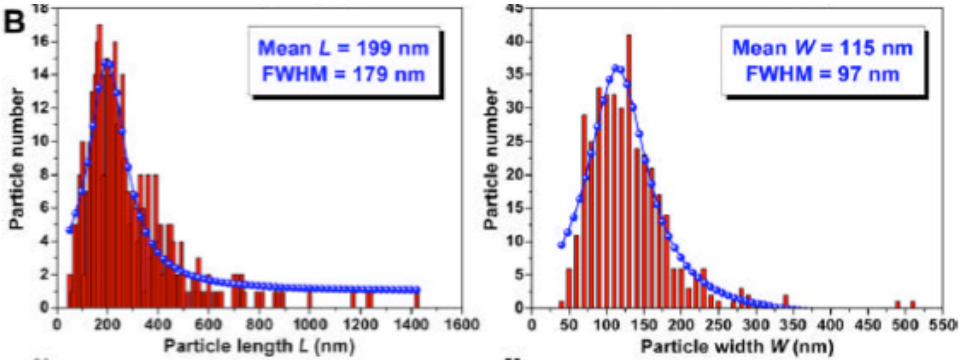

- Small angle X-ray scattering

  Scattering of X-rays by small domains of uniform matter (crystalline or amorphous), for which the electron density ρ^e is different from the continuous medium
  The central peak of scattered intensity gets broader as the domain size (particles, voids) decreases
  SAXS parameters (mean size / size distribution / specific surface area) are derived from analysis of the profile of the SAXS curve

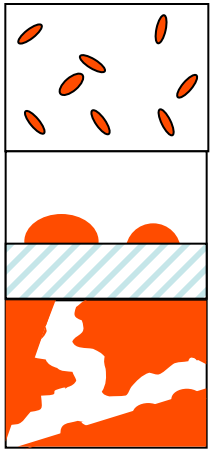

- Mercury porosimetry

  Intrusion of a non-wetting liquid (often Hg) at high pressure, measurement based on the external pressure needed to force the liquid into a pore against the opposing force of the liquid's surface tension, Inner surface of porous materials, pore width > 2nm

Adsorption – driving forces

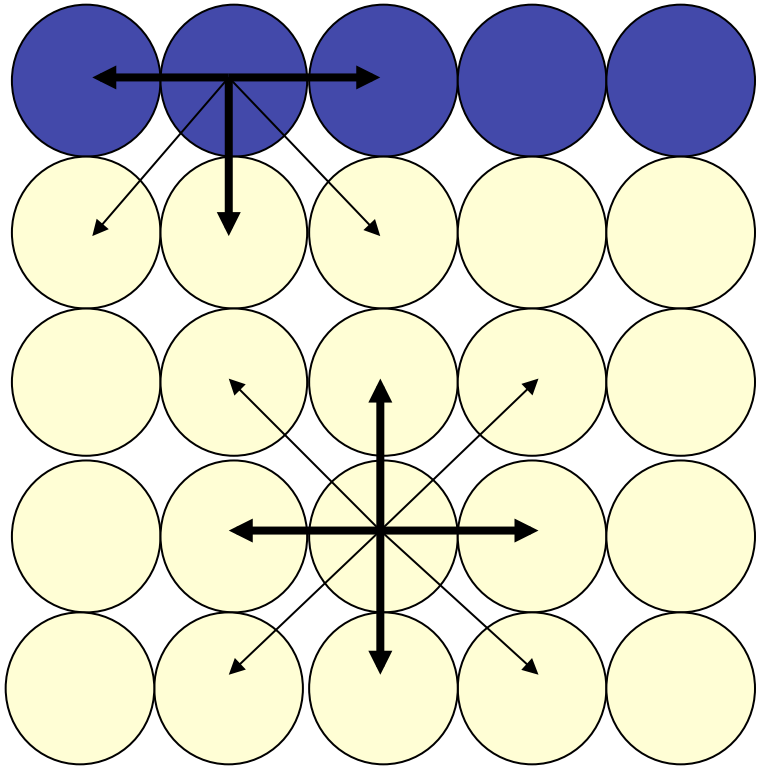

Surface atom – unbalanced forces

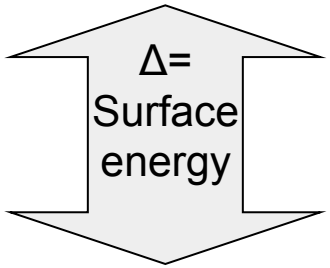

Bulk atom – balanced forces

Adsorption: a substance is enriched at the interface between two phases with respect to its concentration in the homogeneous phase

Involved forces

- ***Formation of a chemical bond (chemisorption)***

- ***Van der Waal´s forces (physisorption)***

1. Dispersion forces* (major part of the interaction potential)
   The electron motion in an atom or molecule leads to a rapidly oscillating dipole moment coupling of two neighboring moments into phase leads to a net attractive potential
2. Ion-dipole (ionic solid/polar gas molecule)
3. Ion-induced dipole (polar solid/polarizable gas molecule)
4. Dipole-dipole (polar solid/polar gas molecule)
5. Quadrupole interactions (symmetrical molecules, e.g., $^{-}O\text{-}C^{++}\text{-}O^{-}$)

* F. London, Z. Phys. 63 (1930) 245.

Similar to forces that lead to liquifidation of vapors

Adsorption

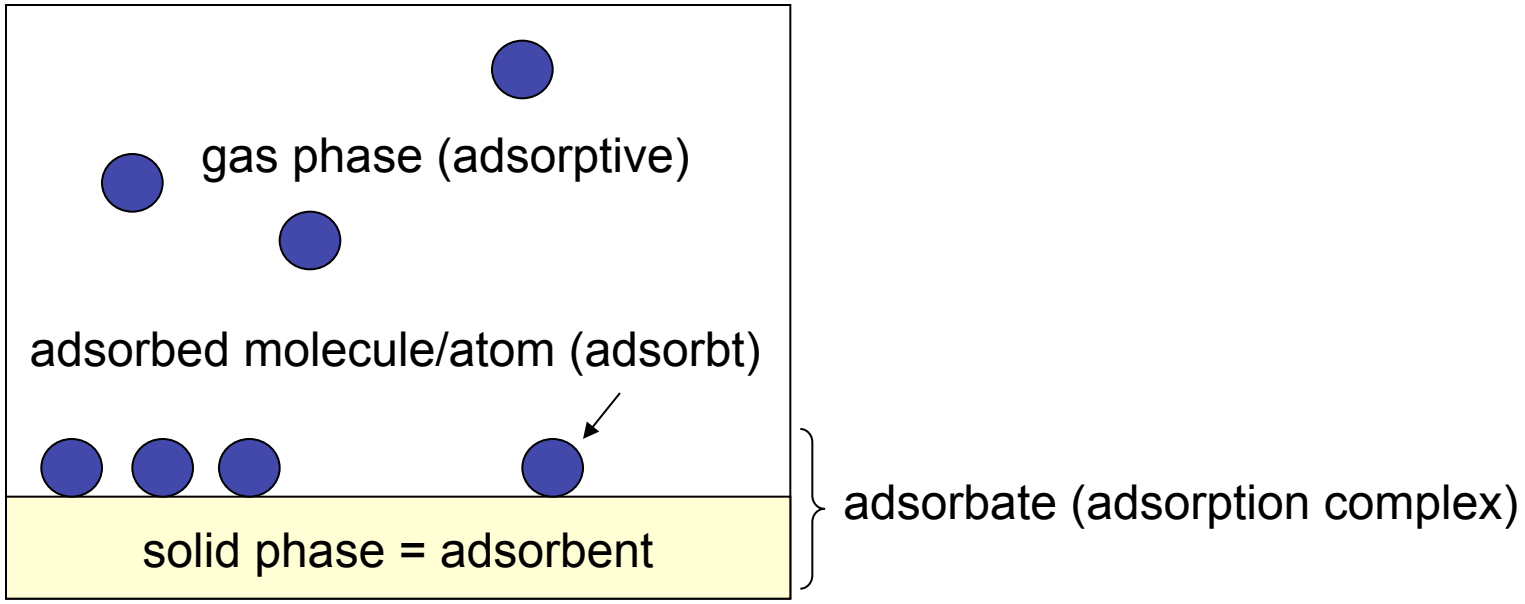
gas phase (adsorptive)
adsorbed molecule/atom (adsorbt)
solid phase = adsorbent
adsorbate (adsorption complex)

Description of adsorption

Relation between T, p, adsorbed amount (surface concentration)

$\Gamma = n_s/s_a$

$\gamma = n_s/m_a$

$\Gamma = \gamma/S_{a,sp.}$

W_s

V_s

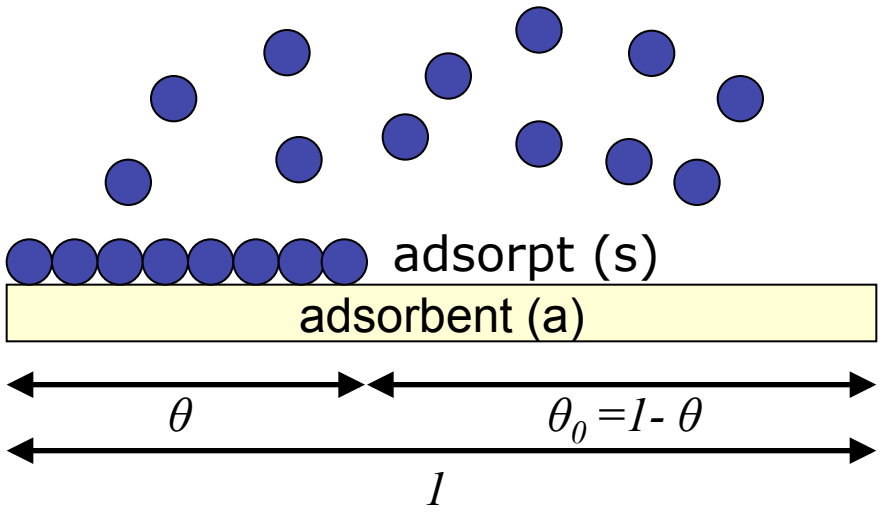

Fraction of occupied surface (coverage)

$\theta = \Gamma/\Gamma_m = \gamma/\gamma_m = N/N_m = W/W_m$

$\Gamma = f(p)$	<eq., T = const.>	adsorption isotherm
$\Gamma = f(T)$	<eq., p = const.>	adsorption isobar
$p = f(T)$	<eq., Γ = const.>	adsorption isostere

Adsorption isotherm

$$\Gamma = f(p)_T$$

Adsorption is favored at lower temperatures

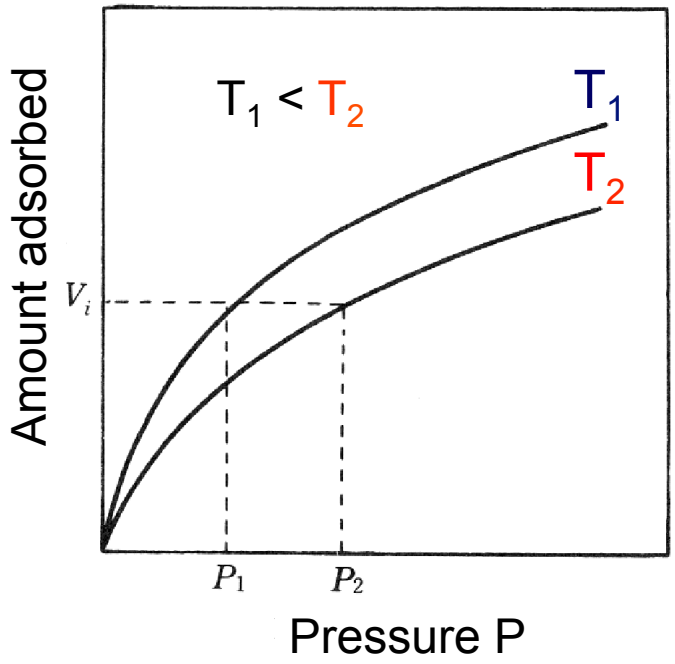

$\Delta G = \Delta H - T\Delta S$

Decrease in translation freedom by adsorption: ΔS<0
Adsorption is a spontaneous process: ΔG<0

↓

ΔH<0 Exothermic process

Volumetric measurement

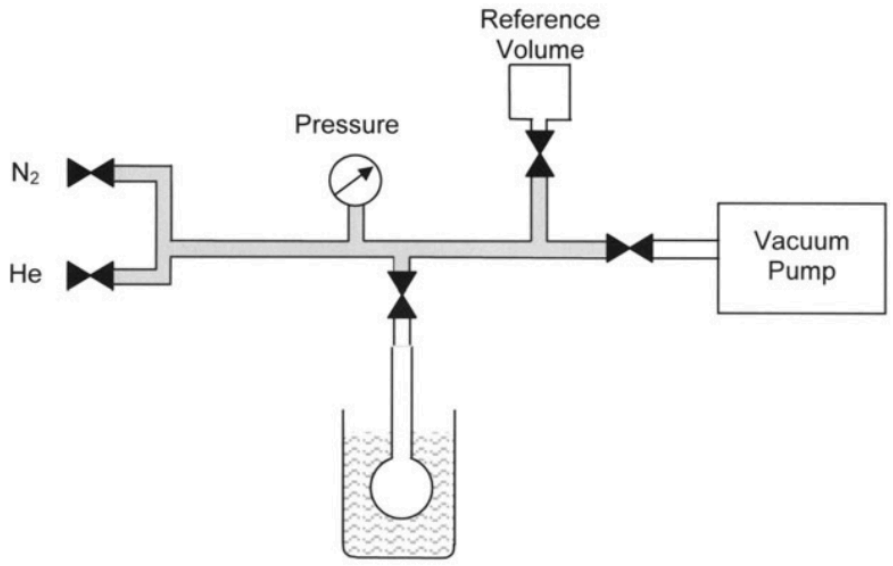

Figure 14.1b Simplified, modern static volumetric apparatus.

V_s volume sorbed
V_d volume of adsorptive dosed
V_m volume of manifold
V_v volume of the sample cell, which is not occupied by the adsorbent
p_m manifold pressure before the dose
p_{eq} equilibrium pressure after the dose
T_{eq} temperature in equilibrium

$$V_d = \left(\frac{p_m V_m}{T_m} - \frac{p_{eq} V_m}{T_{eq}} \right) \times \left(\frac{T_{Std}}{p_{Std}} \right)$$

$$V_s = V_d - \left(\frac{p_{eq} V_{v\,77K}}{p_{Std}} \right)$$

$T_{std} = 273.15\ \mathrm{K}, p_{std} = 760\ \mathrm{torr}$

$V_{stp}[\mathrm{cm}^3] / 22414\ \mathrm{cm}^3 = n_s$

- Application of ideal gas equation
- Void volume determination by He:

(i) He does not adsorb

(ii) He does not penetrate into regions which are inaccessible for the adsorptive

- The pressure is expressed as a fraction of the saturation pressure p_0 that is defined as the saturated equilibrium vapor pressure exhibited by the pure adsorptive contained in the sample at the adsorption temperature
- The saturation pressure depends on the temperature - Clausius-Clapeyron:

$$\ln(p_{0,T2} / p_{0,T1}) = \Delta H / R(1/T_1 - 1/T_2)$$

Volumetric measurement

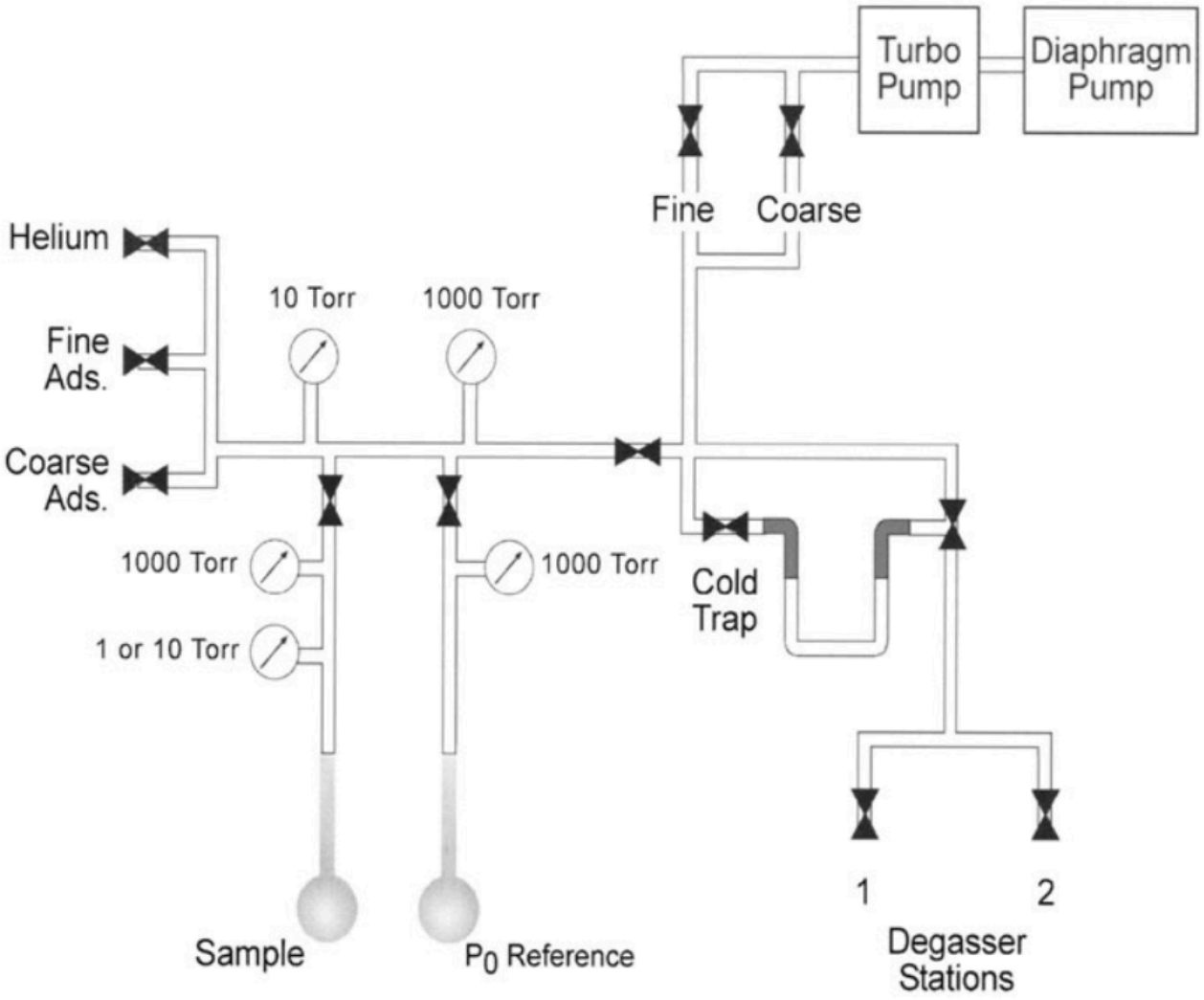

Continuous flow technique (frontal sorption method)

$$N_2O(g) + 2Cu^0{}_s \rightarrow (Cu - O - Cu)_s + N_2(g)$$

$\Delta_R H$ = 317 kJ/mol (N_2O, Cu/ZnO)

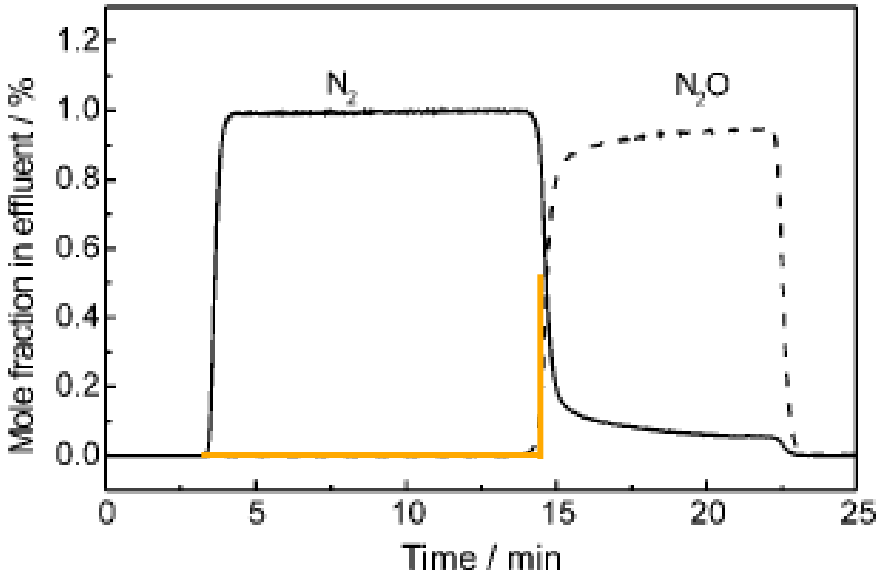

$Cu/ZnO/Al_2O_3$ catalyst

- Flow of 10 Nml/min 1% N_2O/He at 300 K, p=0.1 MPa, m_{cat}=0.2 g bed height=20 mm contact time = 1.4 s **ΔT approx. 1 K**
- Determination of N_2 formed as product of molar flow and peak area by TCD/MS

O. Hinrichsen, T. Genger, and M. Muhler, Chem. Eng. Technol. 23 (2000) 11.

Pulse technique (pulse sorption method)

$$N_2O(g) + 2Cu^0_s \rightarrow (Cu - O - Cu)_s + N_2(g)$$

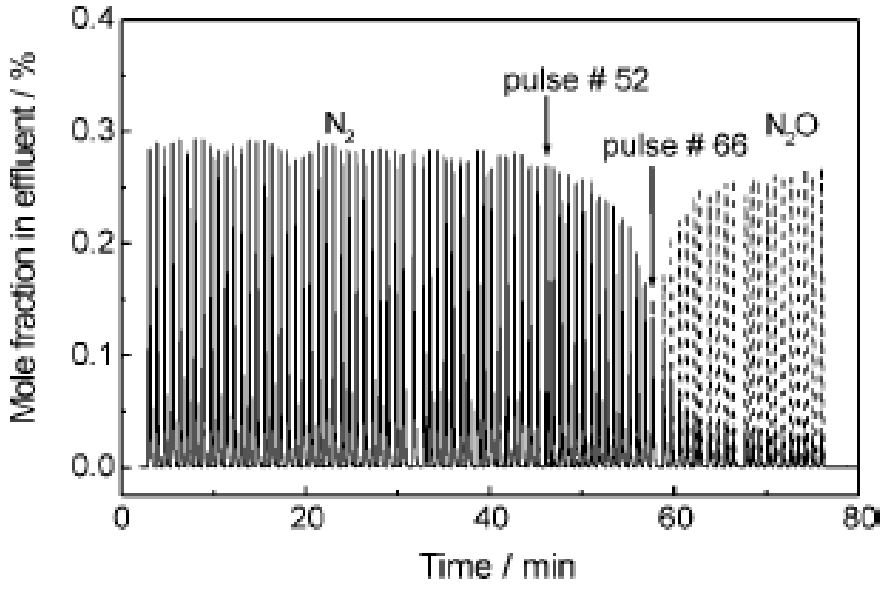

$Cu/ZnO/Al_2O_3$ catalyst

Injection of successive small pulses of known volume into the flow of an inert gas

- Flow of 20 Nml/min He
  V = 1.0 ml N_2O
  T = 300 K
  p=0.1 MPa
- #66= 125 µmol/g N_2

O. Hinrichsen, T. Genger, and M. Muhler, Chem. Eng. Technol. 23 (2000) 11.

Gravimetric techniques

$$CO_2 + 3H_2 \rightleftarrows CH_3OH + H_2O \quad \Delta H_0 = -49.8\ kJ/mol \quad (1)$$

$$CO + 2H_2 \rightleftarrows CH_3OH \quad \Delta H_0 = -91.0\ kJ/mol \quad (2)$$

$$CO_2 + H_2 \rightleftarrows CO + H_2O \quad \Delta H_0 = +41.2\ kJ/mol \quad (3)$$

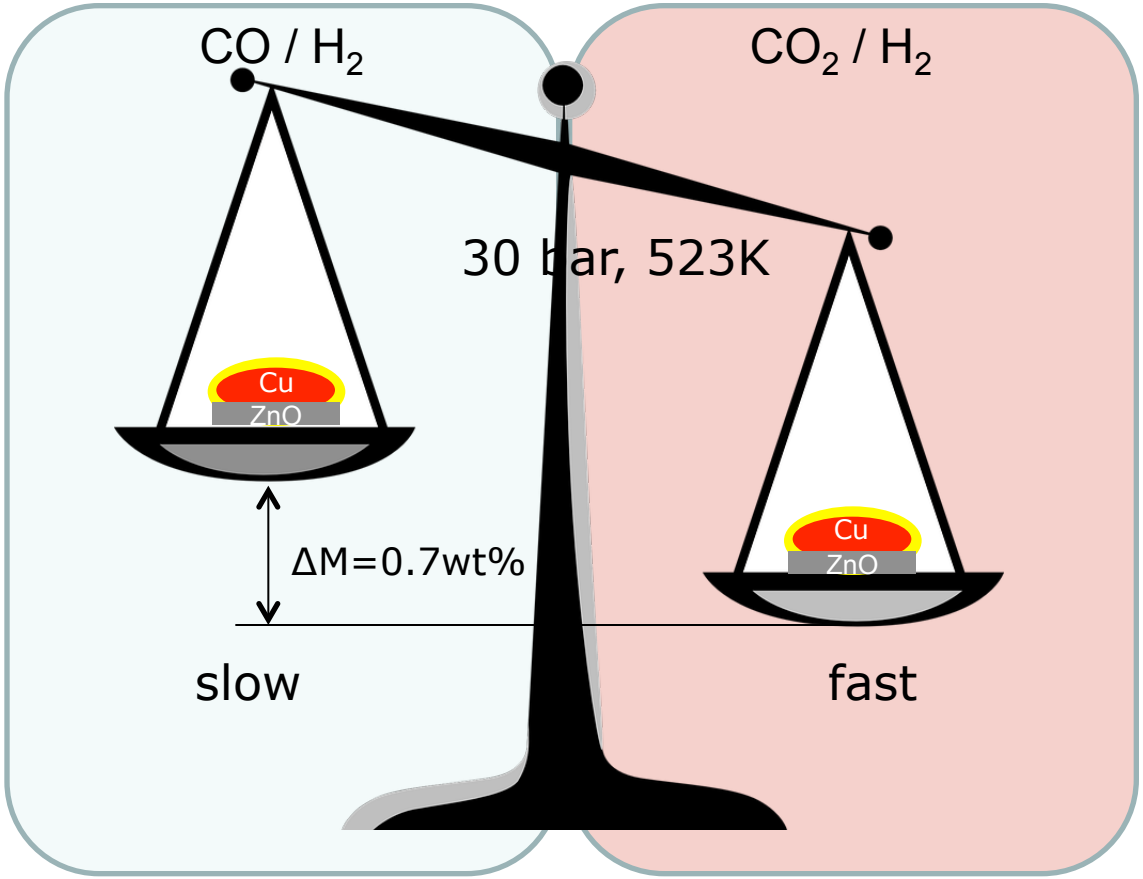

Andrey Tarasov

$$CO_2 + 3H_2 \rightleftarrows CH_3OH + H_2O \quad \Delta H_0 = -49.8\ kJ/mol \quad (1)$$

$$CO + 2H_2 \rightleftarrows CH_3OH \quad \Delta H_0 = -91.0\ kJ/mol \quad (2)$$

$$CO_2 + H_2 \rightleftarrows CO + H_2O \quad \Delta H_0 = +41.2\ kJ/mol \quad (3)$$

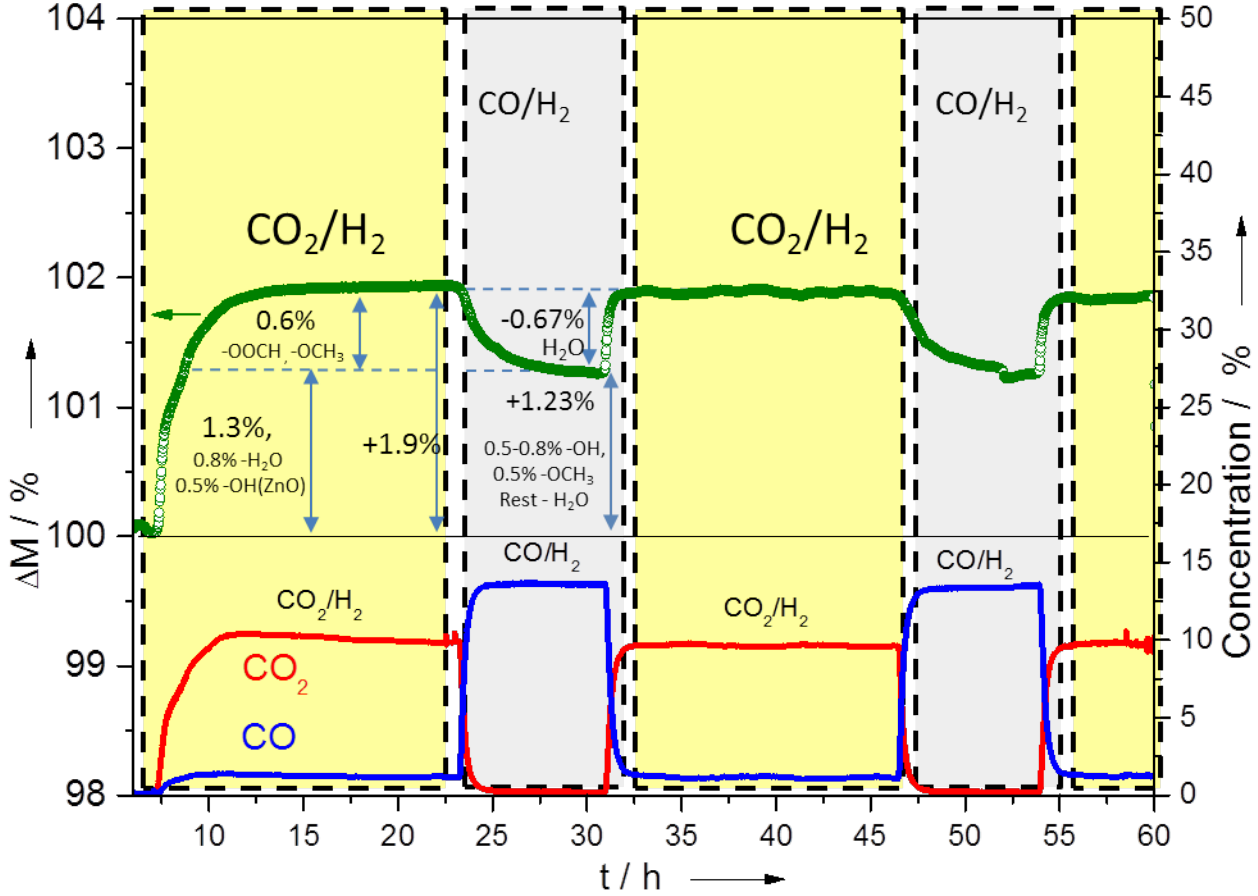

Andrey Tarasov

Adsorption isotherms

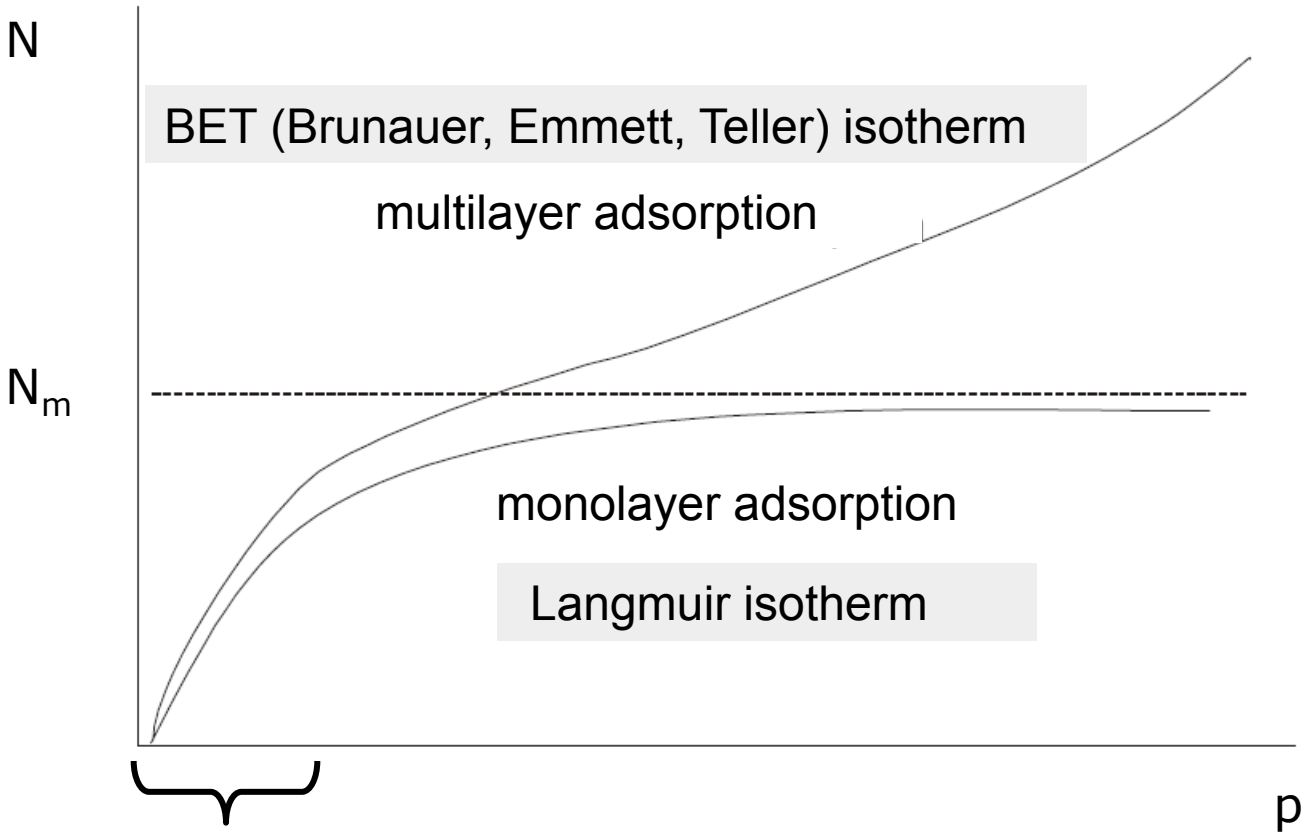

- Freundlich isotherm
  (interaction of adsorbed molecules)
  $\theta = c_1 p^{1/c2}$
- Temkin isotherm
  (adsorption enthalpy is a function of the pressure)
  $\theta = c_1 ln(c_2 p)$

Adsorption isotherm

- Mathematical description of the adsorption isotherms allows to determine
  - Monolayer capacity
  - Surface area
  - Pore data
- The models used for mathematical description are often empirical models that fit more or less to experimental data
- The results are useful and required to interpret catalytic data
- Please consider in the discussion of your results that the surface area or the pore volume determined by using the various empirical models are approximated values

Surface area measurements

$$S = A_x N_m$$

A_x cross-sectional area of the adsorbed molecule

- Nitrogen 0.162 nm^2
- Argon 0.166 nm^2
- Krypton 0.210 nm^2

N_m number of adsorbate molecules required to cover the solid with a single monolayer

Theories that give access to the monolayer capacity using the isotherm

- Langmuir
- BET

Langmuir isotherm*

Assumptions

- Monolayer adsorption
- Energetically uniform surface
- No interactions between adsorbed species - heat of adsorption independent of coverage

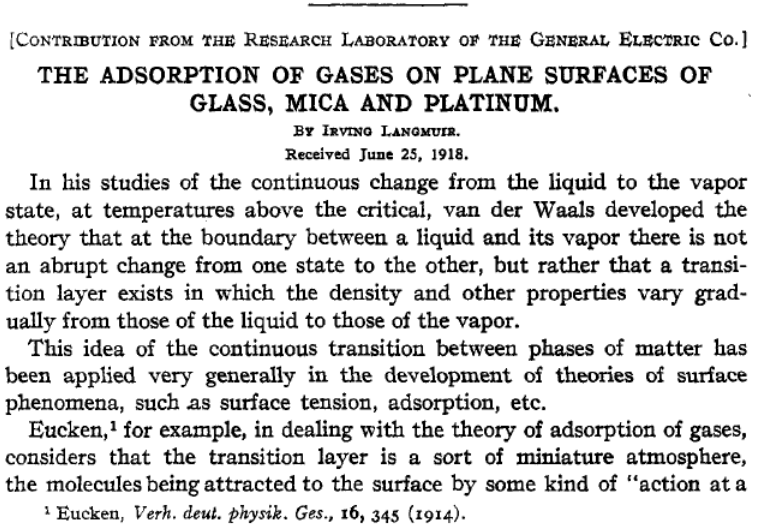

[Contribution from the Research Laboratory of the General Electric Co.]

THE ADSORPTION OF GASES ON PLANE SURFACES OF GLASS, MICA AND PLATINUM.

By Irving Langmuir.

Received June 25, 1918.

In his studies of the continuous change from the liquid to the vapor state, at temperatures above the critical, van der Waals developed the theory that at the boundary between a liquid and its vapor there is not an abrupt change from one state to the other, but rather that a transition layer exists in which the density and other properties vary gradually from those of the liquid to those of the vapor.

This idea of the continuous transition between phases of matter has been applied very generally in the development of theories of surface phenomena, such as surface tension, adsorption, etc.

Eucken,[1] for example, in dealing with the theory of adsorption of gases, considers that the transition layer is a sort of miniature atmosphere, the molecules being attracted to the surface by some kind of "action at a

[1] Eucken, *Verh. deut. physik. Ges.*, **16**, 345 (1914).

Kinetic expression of the adsorption equilibrium

$$r_{ads} = r_{des}$$

$$dN_{ads} = dN_{des}$$

* I. Langmuir, J. Am. Chem. Soc. 40 (1918) 1361.

Langmuir isotherm

$$A + * \underset{k_A^-}{\overset{k_A^+}{\rightleftharpoons}} A^*$$

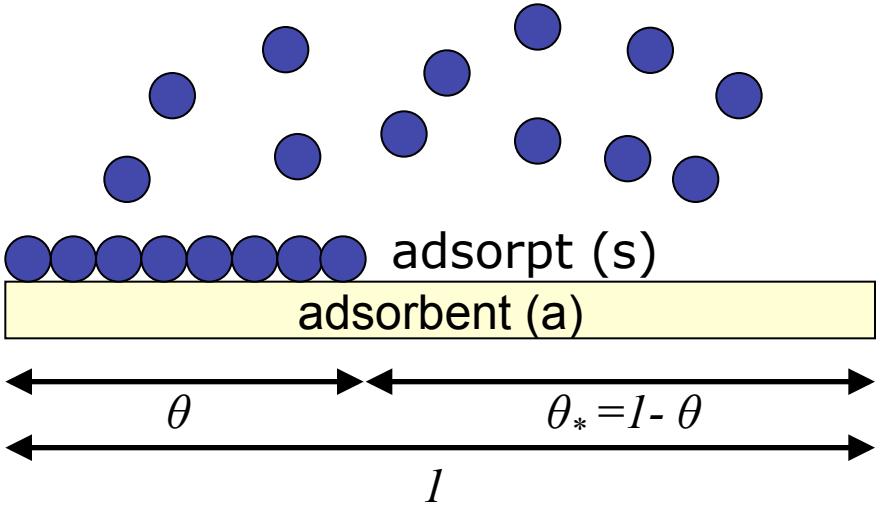

$$\frac{d\theta_A}{dt} = p_A k_A^+ (1-\theta_A) - k_A^- \theta_A$$

$$K_A = \frac{k_A^+}{k_A^-}$$

in equilibrium:

$$p_A k_A^+ (1-\theta_A) = k_A^- \theta_A$$

$$\theta_A = \frac{K_A p_A}{1 + K_A p_A}$$

Irving Langmuir
Nobel Prize in Chemistry in 1932

$$\theta_* = (1-\theta_A) = \frac{1}{1 + K_A p_A} \Rightarrow \theta_A = K_A p_A \theta_*$$

Langmuir isotherm

$$\theta = \frac{N}{N_m} = \frac{K\ p}{1 + K\ p}$$

$$K = \frac{k_{ads}}{k_{des}}$$

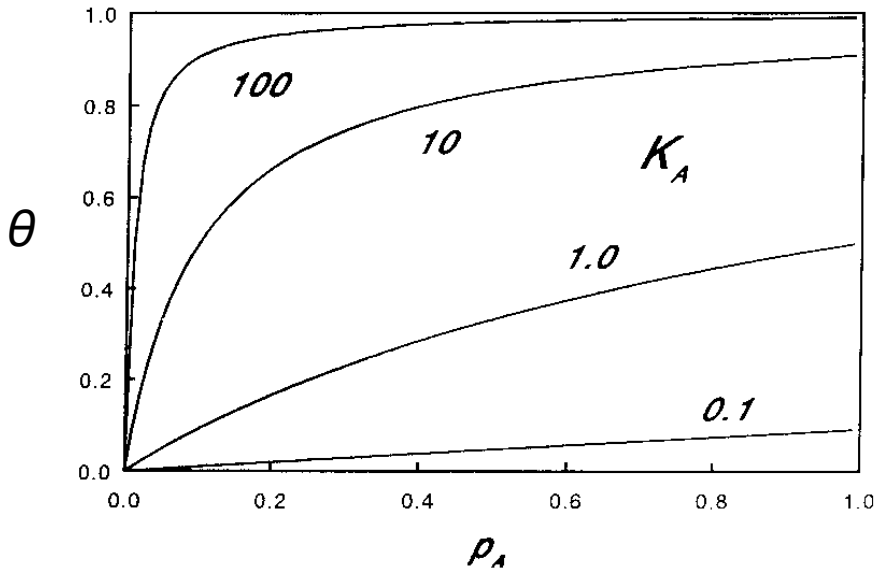

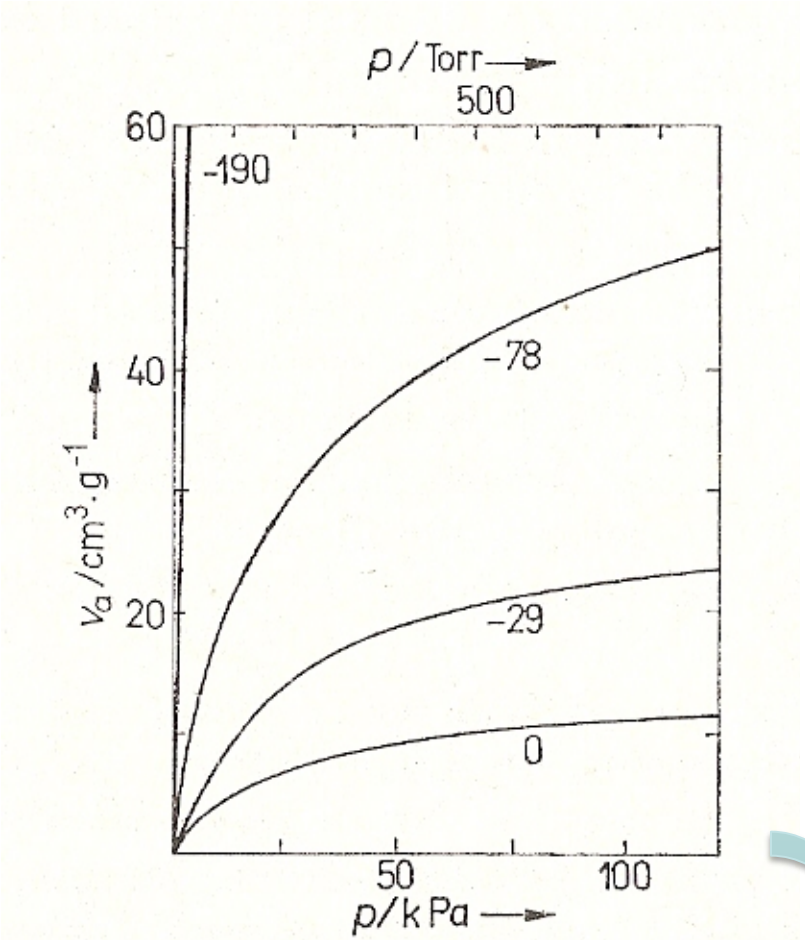

Adsorption of nitrogen on charcoal at different T

$$\left(\frac{\partial \ln K}{\partial T}\right)_{\Theta} = \frac{\Delta_{ads} H}{RT^2}$$

Langmuir isotherm

$$\theta = \frac{N}{N_m} = \frac{K\ p}{1 + K\ p}$$

Linear plot

$$\frac{p}{N} = \frac{1}{KN_m} + \frac{p}{N_m}$$

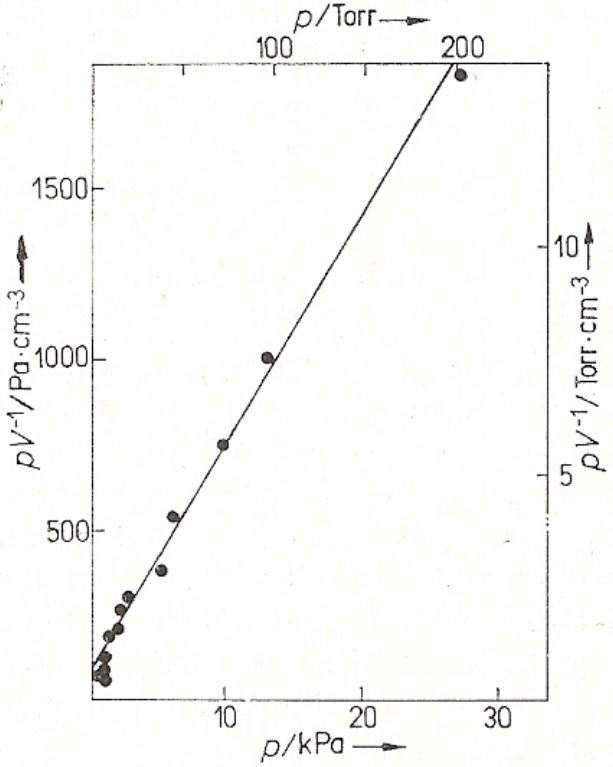

Abb. 6.47
Linearisierte Langmuirsche Adsorptionsisotherme für die Adsorption von Wasserstoff an Kupferpulver bei 25 °C

$$n = \frac{N}{N_A} = \frac{m_m}{M_{asdorptive}}$$

$$S = N_m A_x = \frac{m_m N_A A_x}{M_{asdorptive}}$$

Langmuir isotherm – adsorption of propane on oxides

M. Hävecker *et al.*, Journal of Catalysis 285 (2012) 48–60.

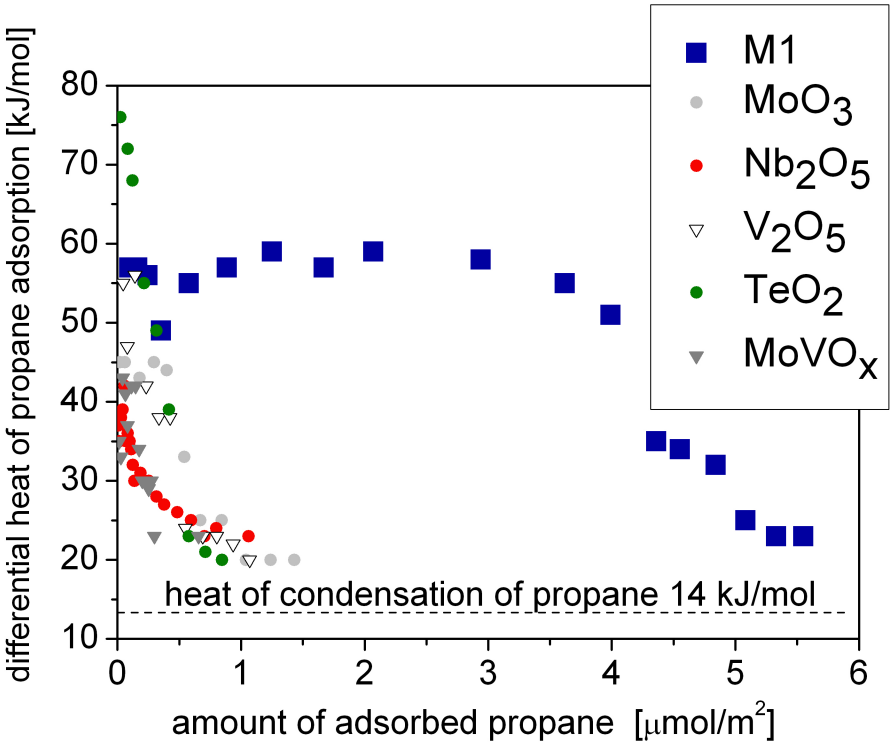

Adsoption isotherm of propane over M1 at T=313 K

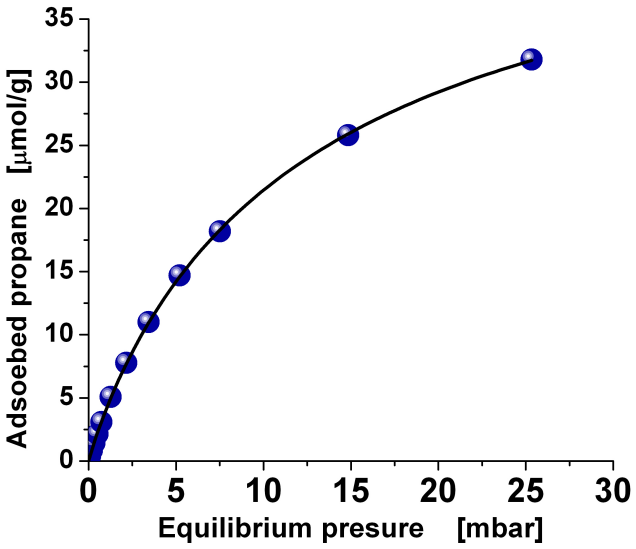

Cross-sectional area of propane: 36 Å^2

$K = 0.111(6)\ hPa^{-1}$

$N_m = 43\ \mu mol\ g^{-1}$

$S_{Langmuir} = 9.2\ m^2\ g^{-1}$

$S_{BET} = 8.8\ m^2\ g^{-1}$

A.L. McClellan, H.F. Harnsberger, J. Colloid Interface Sci. 23 (1967) 577.
S.J. Gregg, R. Stock, Trans. Faraday Soc. 53 (1957) 1355.

Other isotherms – C_3H_8 adsorption on CNTs - Temkin

B. Frank *et al.*, ChemPhysChem 12 (2011) 2709 – 2713.

$$\theta = \frac{RT}{q_{ads}^{(\theta=0)} - q_{ads}^{(\theta=1)}} \ln\left(\frac{1 + \frac{p}{p^*}\exp\frac{q_{ads}^{(\theta=0)}}{RT}}{1 + \frac{p}{p^*}\exp\frac{q_{ads}^{(\theta=1)}}{RT}}\right)$$

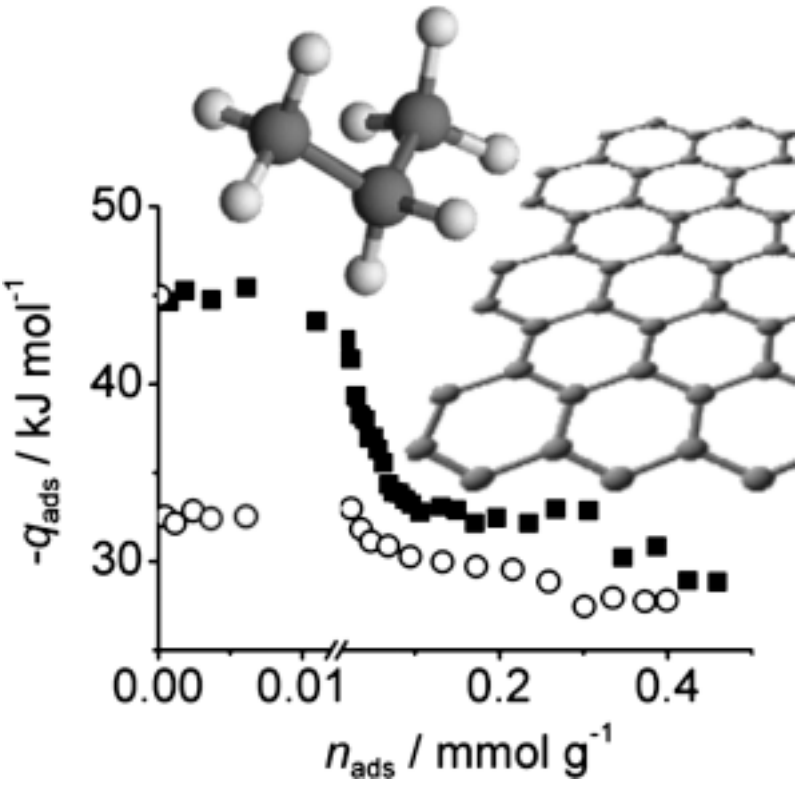

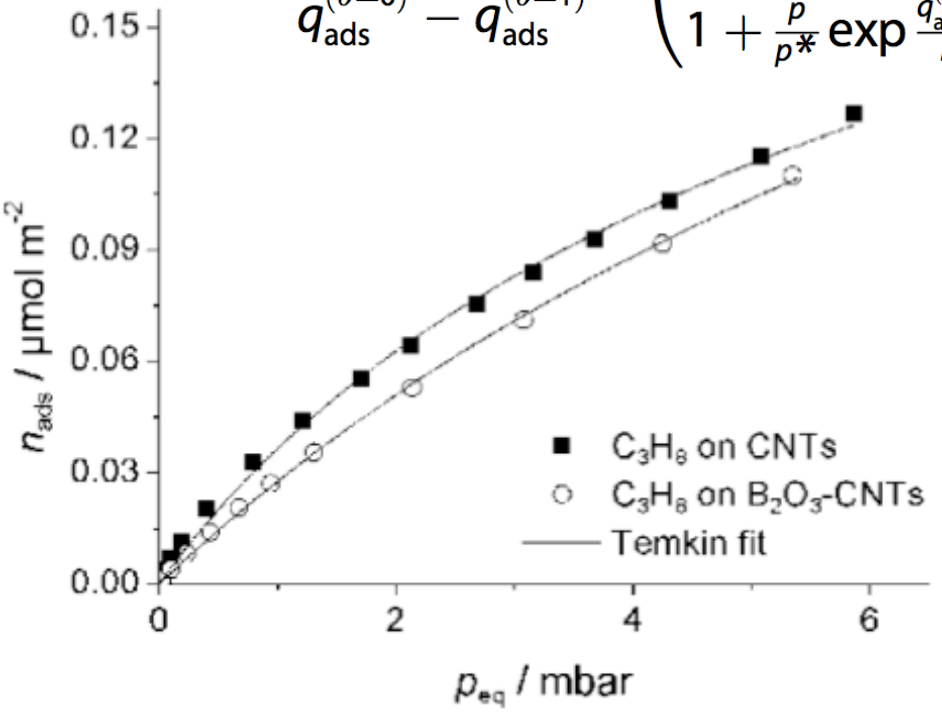

Figure 3. Isotherms of propane adsorption (313 K) on the oxygen surface groups of CNT and B_2O_3–CNT catalysts used in ODH of propane.

M. I. Temkin, Zhur. Fiz. Khim. 15 (1941) 296.

Adsorption isotherms

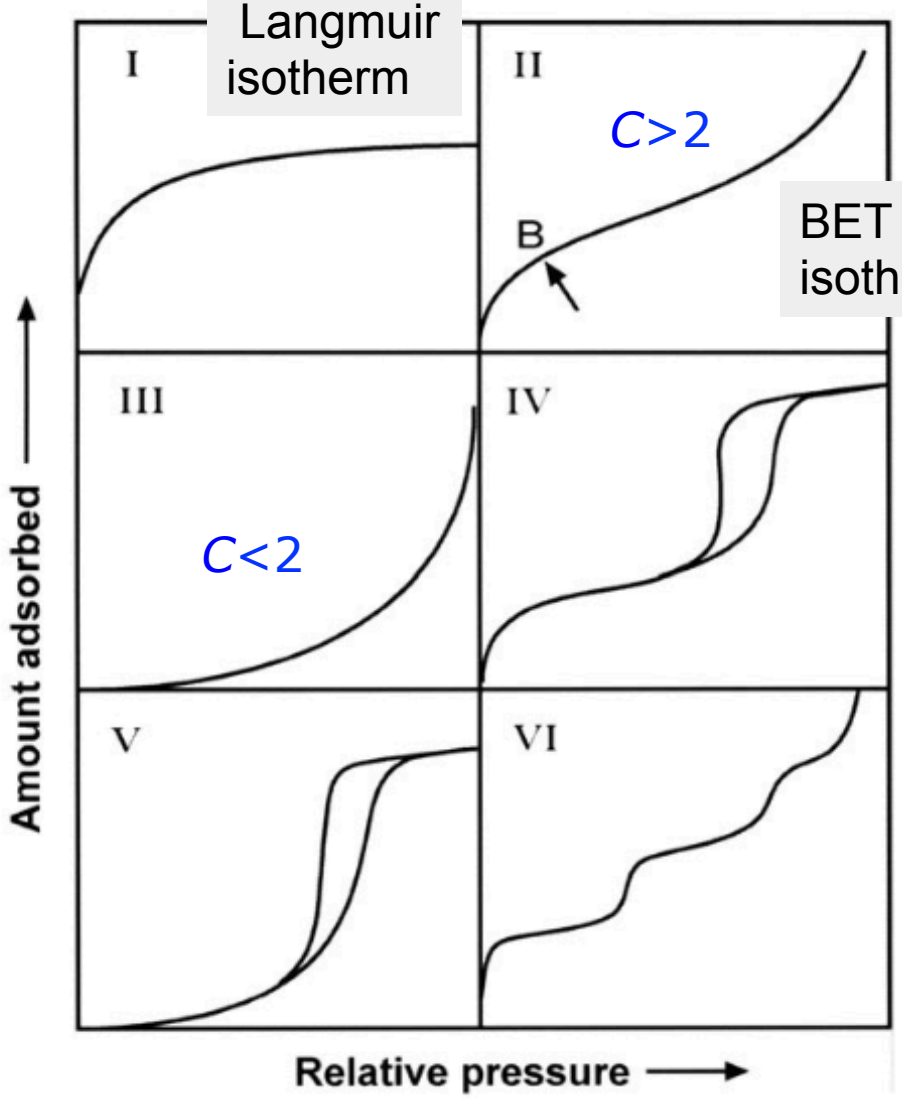

Langmuir isotherm

BET (Brunauer, Emmett, Teller) isotherm

C BET constant

Sing, K. S. W., Reporting physisorption data for gas/solid systems with special reference to the determination of surface area and porosity. *Pure and Applied Chemistry* **1985,** *57*, 603-619.

Figure 3.2 IUPAC classification of sorption isotherms. From [1].

BET isotherm (Brunauer, Emmett, Teller)*

[CONTRIBUTION FROM THE BUREAU OF CHEMISTRY AND SOILS AND GEORGE WASHINGTON UNIVERSITY]

Adsorption of Gases in Multimolecular Layers

BY STEPHEN BRUNAUER, P. H. EMMETT AND EDWARD TELLER

Introduction

The adsorption isotherms of gases at temperatures not far removed from their condensation points show two regions for most adsorbents: at low pressures the isotherms are concave, at higher pressures convex toward the pressure axis. The higher pressure convex portion has been variously interpreted. By some it has been attributed to condensation in the capillaries of the adsorbent on the assumption that in capillaries of molecular dimensions condensation can occur at pressures far below the vapor pressure of the liquid. By others such isotherms are believed to indicate the formation of multimolecular adsorbed layers. DeBoer and Zwicker[1] explained the adsorption of non-polar molecules on ionic adsorbents by assuming that the uppermost layer of the adsorbent induces dipoles in the first layer

I. The Polarization Theory of DeBoer and Zwicker

According to DeBoer and Zwicker, the induced dipole in the ith layer polarizes the $i + 1$st layer, thus giving rise to induced dipole moments and binding energies that decrease exponentially with the number of layers. If we call the dipole moment of a molecule in the i-th layer μ_i, it follows that

$$\mu_i = c_1 C^i \qquad (1)$$

where c_1 and C are appropriate constants, C actually being equal[3] to μ_i/μ_{i-1}. The corresponding binding energy is proportional to the square of the dipole moment

$$\phi_i = c_2 C^{2i} \qquad (2)$$

where c_2 is another constant. The equilibrium pressure of the nth layer (top layer), p_n, according to Boltzmann's law varies exponentially with the

* S. Brunauer, P.H. Emmett, E. Teller, J. Am. Chem. Soc. 60 (1938) 309.

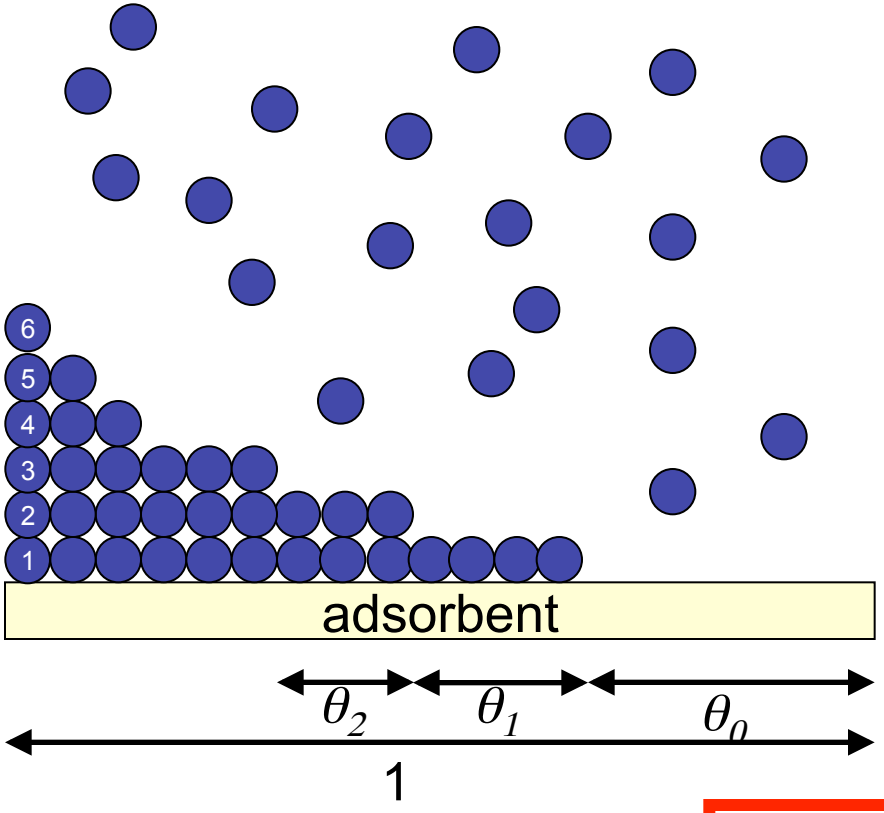

Description of all isotherm types

Assumptions

- Multilayer adsorption
- First layer: Langmuir adsorption
- Second and further layers: condensation of gas onto liquid
- Heat of adsorption:

  First layer > second layer = … = …= heat of condensation

$$\theta = \frac{N}{N_m} = \frac{C \cdot (p/p_0)}{(1 - p/p_0) \cdot [1 - p/p_0 + C(p/p_0)]}$$

p_0 …vapor pressure of liquid N_2

* S. Brunauer, P.H. Emmett, E. Teller, J. Am. Chem. Soc. 60 (1938) 309.

$$\frac{1}{W\left[p/p_0 - 1\right]} = \frac{1}{W_m C} + \frac{C-1}{W_m C}\left(\frac{p}{p_0}\right)$$

W ... mass of adsorbed N_2

Relative pressures near completed monolayers

$0.05 < p/p_0 < 0.3$

$$W_m = \frac{1}{s+i}$$

$$C = \frac{s}{i} + 1$$

$$s = \frac{C-1}{W_m C}$$

$$i = \frac{1}{W_m C}$$

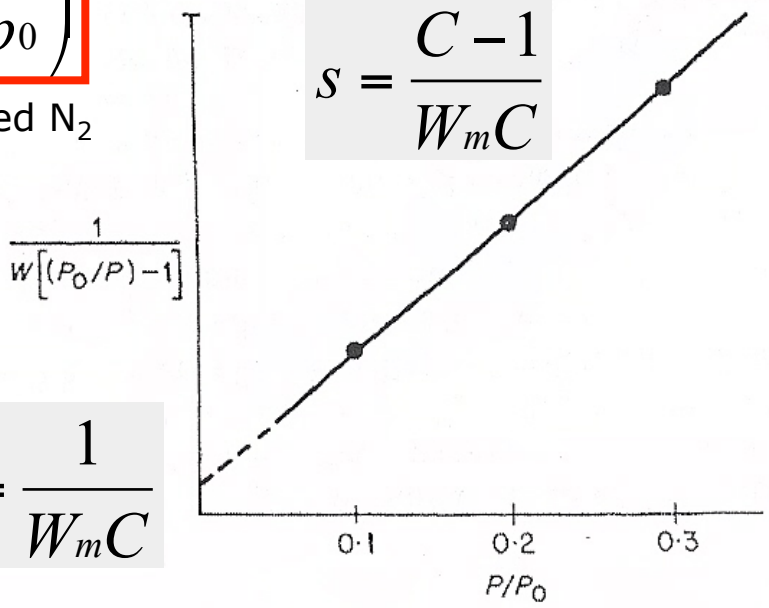

$$S = \frac{W_m N_A A_x}{M_{adsorptive}}$$

$$S_{sp.} = \frac{S}{m}$$

Single point BET

Assumption: For high values of C the intercept may be taken as zero

$$W_m = W\left(1 - \frac{p}{p_0}\right)$$

$$S = W\left(1 - \frac{p}{p_0}\right)\frac{N_A}{M_{adsorptive}} A_x$$

„Monolayer" coverage

$$\theta_0 = \frac{\sqrt{C} - 1}{C - 1} = \left(\frac{p}{p_0} \right)_m$$

$$C = 100$$

$$\theta_0 = \frac{\sqrt{100} - 1}{100 - 1} = 0.091$$

- The adsorbate is not necessarily arranged in neat stacks of various hight
- The numerical value of the relative pressure at which $W = W_m$ corresponds to the fraction of surface unoccupied by the adsorbate

The BET constant

$$\frac{W}{W_m} = \left(1 - \frac{p}{p_0}\right) + \frac{1}{C}\left(\frac{p}{p_0} + \frac{p_0}{p} - 2\right)$$

Table 5.3 Values of W/W_m and relative pressures for various values of C.

P/P_0	C = 0.05	C = 0.5	C = 1	C = 2	C = 3	C = 10	C = 100	C = 1000
0.02	0.001	0.010	0.020	0.040	0.059	0.173	0.685	0.973
0.05	0.003	0.027	0.052	0.100	0.143	0.362	0.884	1.030
0.10	0.006	0.058	0.111	0.202	0.278	0.585	1.020	1.100
0.20	0.015	0.139	0.250	0.417	0.536	0.893	1.200	1.250
0.30	0.030	0.253	0.429	0.660	0.804	1.160	1.400	1.430
0.40	0.054	0.417	0.667	0.952	1.110	1.450	1.640	1.660
0.50	0.095	0.667	1.000	1.330	1.500	1.820	1.980	2.000
0.60	0.172	1.060	1.490	1.870	2.040	2.340	2.480	2.500
0.70	0.345	1.790	2.330	2.740	2.910	3.190	3.320	3.330
0.80	0.833	3.330	4.000	4.440	4.620	4.880	4.990	5.000
0.90	3.330	8.330	9.090	9.520	9.680	9.900	9.990	10.000
0.94	7.350	14.700	15.700	16.200	16.300	16.600	16.700	16.700

Applicability of the BET theory

- In the region of relative pressures near completed monolayers ($0.05<p/p_0<0.3$) experiment and theory agree well → powerful method of surface area determination
- In the linear BET range the very high energy sites are occupied and extensive multilayer coverage has not yet commenced
- $C<2$: Better change the adsorbate

$$C = e^{(\Delta_{des}H - \Delta_{evac}H/RT)}$$

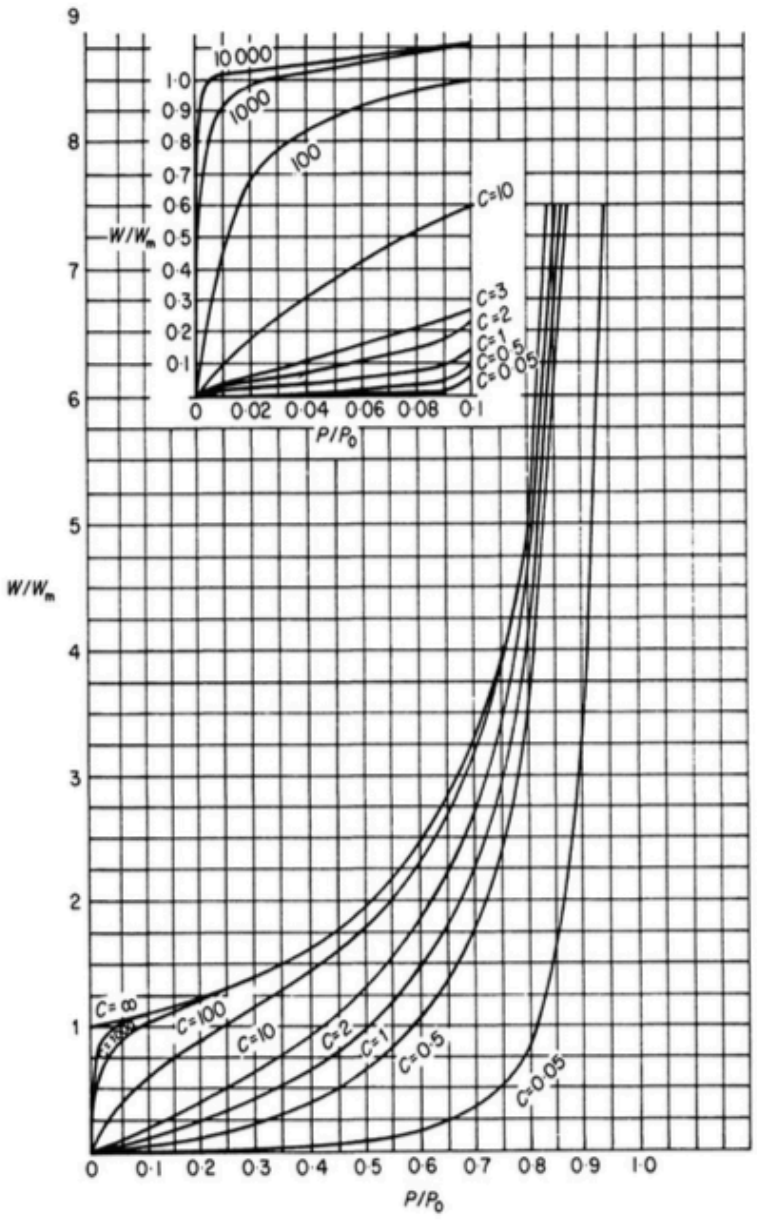

Figure 5.3 Isotherm shapes as a function of BET C values.

Applicability of the BET theory

- BET theory ignores inhomogeneities of the surface and lateral adsorbate adsorbate interactions
  - *High energy sites will be occupied at lower relative pressures*
  - *Reason for the nonlinearity of BET plots at $p/p_0 < 0.05$*
- Polarization forces would induce a higher heat of adsorption in the second layer than in the third and so forth
  - *Reason for the failure of the BET equation at $p/p_0 > 0.3$*
- The BET equation is applicable for surface area analysis of nonporous materials
  - *Difficulties to separate mono-multilayer adsorption from pore filling*
  - *Filling of **micropores** is completed at $p/p_0 < 0.1$, however, linear BET plot are found at even lower relative pressures*
  - *→ measured surface area reflects not a real internal surface, but a „characteristic" BET surface area*
  - *For **mesoporous materials** exhibiting pore diameters between **2 and 4 nm (MCM-41, MCM-48)** pore filling is observed at pressures close to mono-multilayer formation*
  - *→ overestimation of monolayer capacity*

Cross-sectional area

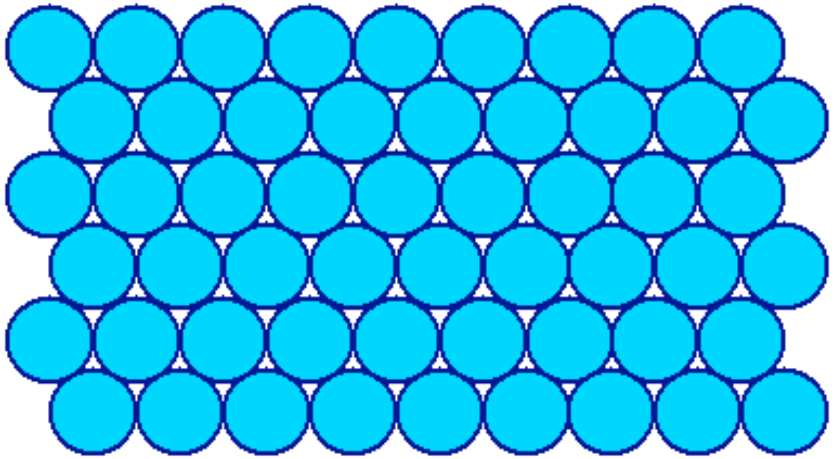

Closed-packed hexagonal arrangement of spheres

$$A_x = 1.091\left(\frac{\overline{V}}{\overline{N}}\right)^{\frac{2}{3}} \times 10^6$$

$\overline{V}$ liquid molar volume

$\overline{N}$ Avogadro's number

$(6.022 \times 10^{23}$ molecules per mole)

Nitrogen as the standard adsorptive

- The cross sectional area depends on T, adsorbate-adsorbate, and adsorbent-adsorbate interactions
- For most of the adsorbents the C constant for N_2 lies in the range from about 50 to 300 (no very weak interaction, no chemisorption)
- Its permanent quadrupole moment is responsible for the formation of well-defined monolayers on most of the surfaces
- Overestimation (20%!) of surface areas of hydroxylated silica surfaces due to specific interactions with the polar surface groups (use 13.5 Å^2)

Langmuir, 1994, 10 (11), pp 4225–4231.

Cross-sectional area

Table 5.4 Cross-sectional areas of some frequently used adsorptives.

Adsorptive	Temperature	Cross-sectional area ($Å^2$)[15]	Customary Value ($Å^2$)	
Nitrogen	77.35 K	13.0 - 20.0	16.2	
Argon	77.35 K	10.0 - 19.0	13.8	6.5 K below bulk triple point
Argon	87.27 K	9.7 - 18.5	14.2	
Krypton	77.35 K	17.6 - 22.8	20.2	
Xenon	77.35 K	6.5 - 29.9	16.8	
Carbon Dioxide		14 - 22.0		
	195 K		19.5	
	273 K		21.0	
Oxygen	77.35 K	13 - 20	14.1	
Water	298.15 K	6 - 19	12.5	
n-Butane	273.15 K	36 - 54	44.4	
Benzene	293.15 K	73 - 49	43.0	

Low surface area analysis

- With nitrogen it is possible to measure absolute surface areas as low as

  0.5-1 m^2

- To measure lower surface areas the ratio between the number of molecules in the void volume and adsorbed molecules must be reduced
- Super-cooled liquid Kr (77 K) has a saturation pressure of 2.63 torr, i.e., the number of molecules in the free space of the sample cell is significantly reduced compared to nitrogen (1/300th)
- Cross sectional area of Kr varies depending on the adsorbent surface / wetting behavior in “solid” state
- But krypton has been established for low surface area measurements (0.5-0.05 m^2)

Capillary condensation in mesopores (2 – 50 nm)

Capillary condensation

Phenomenon whereby a gas condenses to a liquid-like phase in a pore at a pressure p less than saturation pressure p_0 of the bulk liquid

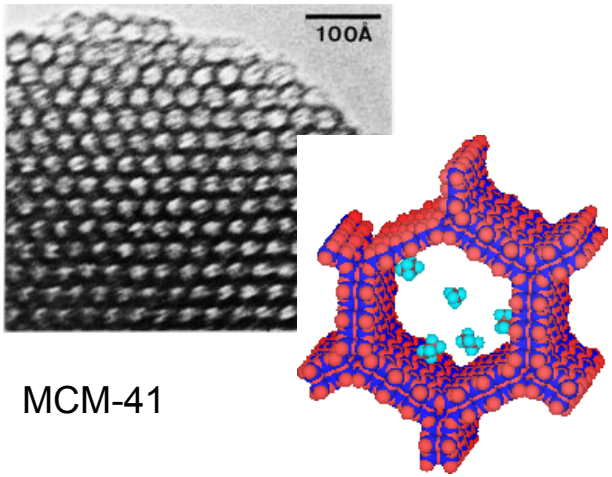

MCM-41

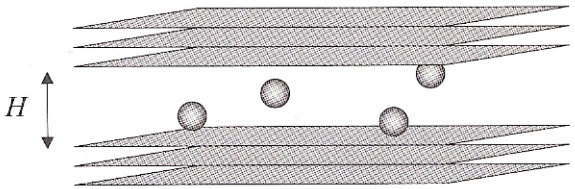

Fig. 3. The slit pore model. Each layer represents a graphene layer.

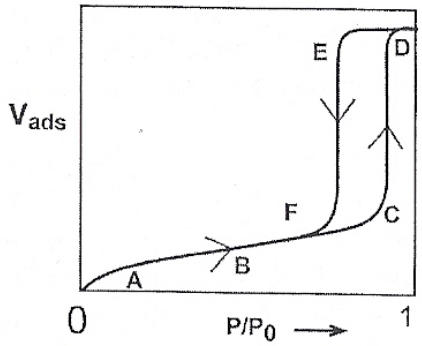

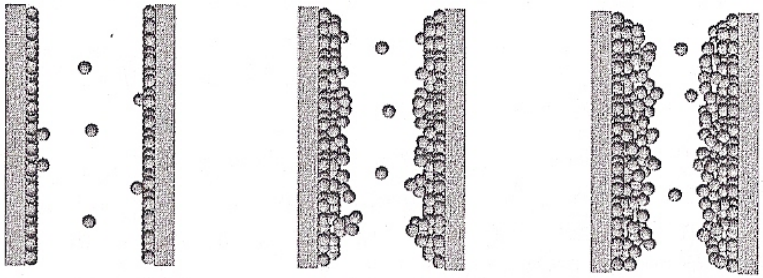

A Monolayer formation | B Multilayer adsorption | C Critical film thickness reached

D Capillary condensation | E Pore evaporation | F multilayer film

The wider the pore size distribution the less sharper is the pore condensation step

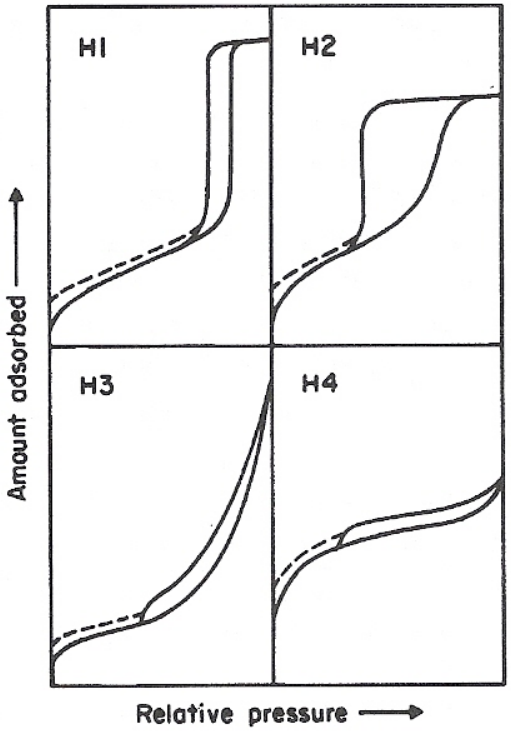

Fig. 3. Types of hysteresis loops

H1 well defined cylyndrical pore channels

H2 disordered pores
(pore blocking, percolation phenomena)

H3 non-rigid aggregates of plate-like particles
(slit-shaped pores)

H4 narrow slit pores including pores in the micropore region

Low pressure hysteresis
no accurate pore size analysis possible!

- Changes in the volume of the adsorbent
  - Swelling of non-rigid pores
- Irreversible uptake of molecules in the pores
- Chemisorption

* K.S.W. Sing et al., Pure Appl. Chem. 57 (1985) 603.

The relative pressure where the pore condensation occurs depends on the pore radius

The Kelvin equation provides a correlation between pore radius and pore condesation pressure

Assumptions

- Pores of cylindrical shape
- No fluid-wall interactions

$$\ln\frac{p}{p_0} = \frac{-2\gamma V_l}{r_p RT}$$

γ surface tension of liquid nitrogen
V_l liquid molar volume
r_p pore radius
r_k critical radius
R universal gas constant
t statistical thickness

$$r_k = \frac{4.15}{\log(p_0/p)}\ \text{Å} \qquad (N_2,\ 77\ K)$$

$$r_p = r_k + t$$

$$t = 3.54\left[\frac{5}{\ln(p/p_0)}\right]\ \text{Å}$$

- The depth of the adsorbed multilayer film present prior to condensation is expressed in form of the statistical thickness *t* (number of layers times thickness of one layer)
- The thickness of one closed-packed hexagonal N_2 layer is 3.54 A
- *t* is a function of the relative pressure
- The empirical equation depends on the adsorbent

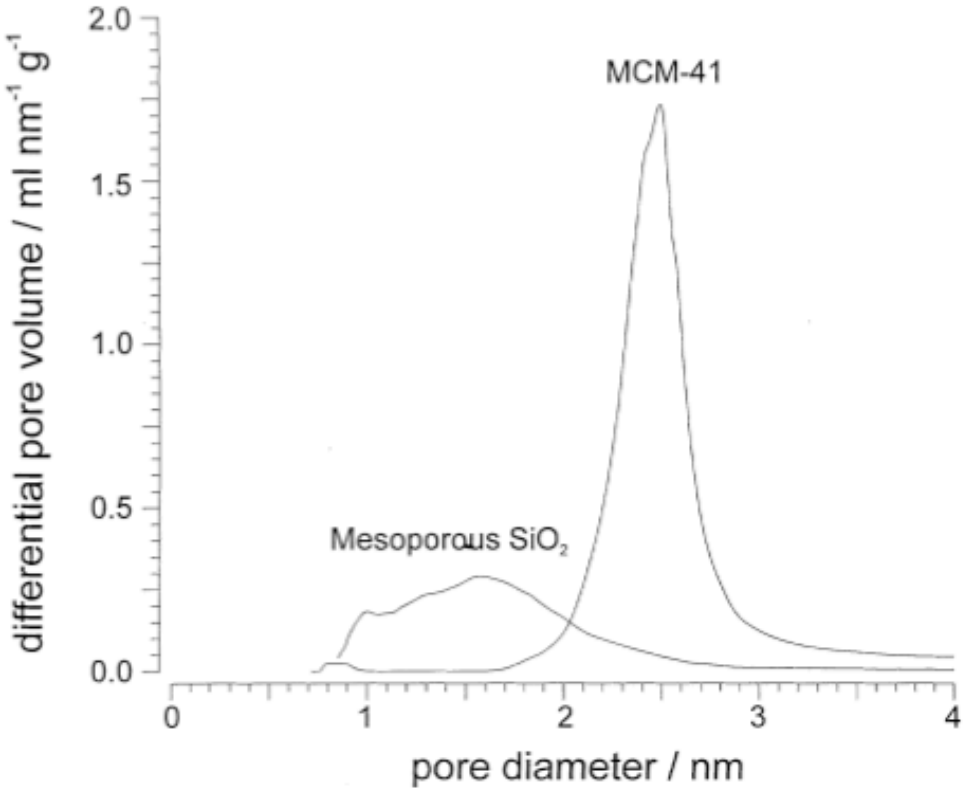

Fig. 3. Pore-size distribution according to the BJH method.

S. Storck et al. / Applied Catalysis A: General 174 (1998) 137-146.

The shape of the isotherm does not depend only on the texture of the porous material, but also on the differences of the thermodynamic states between the confined fluid and the bulk fluid

H1 - independent cylindrical pores (MCM-41, SBA-15)

„Independent pore model“

- Pore condensation is associated with metastable states of the pore fluid in ordered materials
- The **desorption branch** of the hysteresis loop reflects the equilibrium phase transition
- Methods, which describe the equilibrium phase transition (**BJH**) have to be applied to the desorption branch
- Applicable also to three-dimensional network of pores

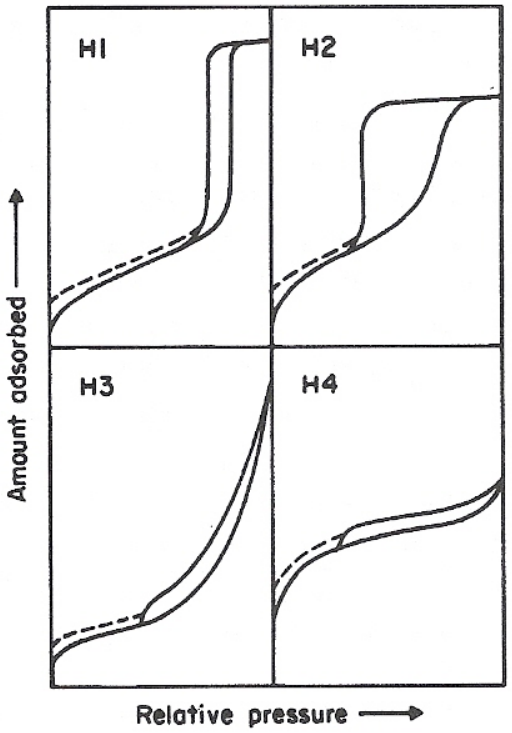

Fig. 3. Types of hysteresis loops

H2, H3 – disordered, connected pores

- Origin of hysteresis not yet completely understood
- Pore blocking (inkbottle pores) associated with the desorption process
- Analysis of the **adsorption branch** (**NLDFT**-spinodal condensation method, Kelvin equation based approach calibrated for the adsorption branch)

Tensile Strength Effect (TSE)

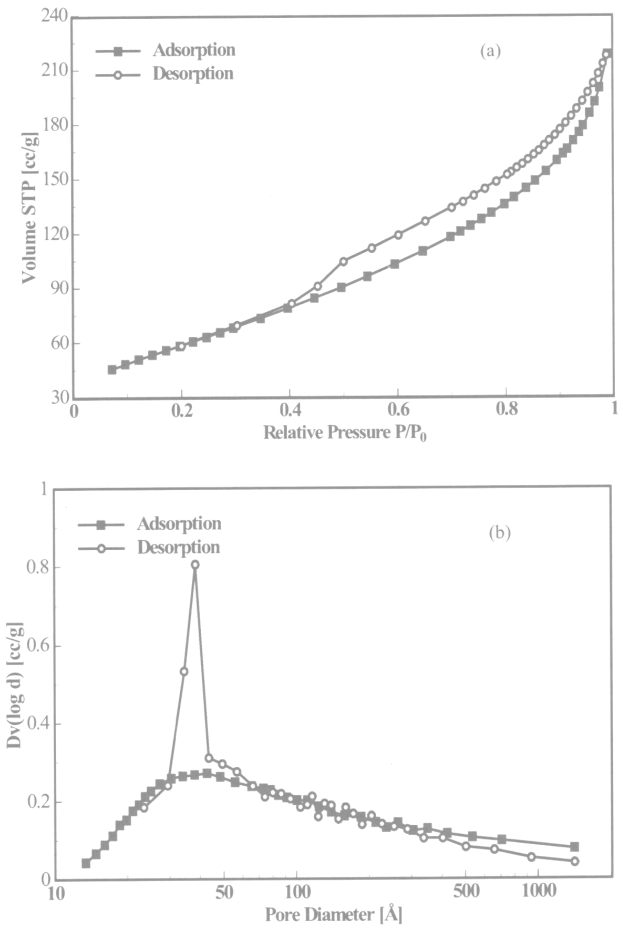

Figure 8.7 (a) Nitrogen adsorption/desorption at ~77 K on a disordered alumina catalyst; (b) BJH pore size distribution curves from adsorption and desorption branches.

Table 2
Examples of erroneous assignment of the TSE to real pores at approximately 3.8 nm

System	Peak position in PSD (nm)	Comments in original manuscript	Ref.
ZSM-5 zeolite with uniform 4 nm pores	**4**	Creation of uniform 4 nm pores upon alkaline treatment of ZSM-5 zeolite	[26]
Dealuminated Al-rich zeolites	**3.8**	Narrow peaks suggesting homogeneous pore sized system around 4 nm	[75]
V-MCM-41 and Cr-MCM-41 with hierarchical structure	2.5–2.7, **3.9**	Bimodal PSD in V-MCM-41 and Cr-MCM-41 by simultaneously growing of two types of micelles	[76]
Thermally stable MCM-41 with complementary textural porosity	2.5–2.6, **3.6**	Bimodal framework and textural PSDs suggesting complementary porosity	[77]
Vanadium-doped MCM-41	2–3, **3.8**	V-MCM-41 with bimodal PSD, only the smaller diameter being variable	[78]
Novel aluminosilicate with bimodal mesopore distribution	2.6, **3.8**	Novel aluminosilicate with bimodal PSD and possible application in catalysis and separations	[79]
Micro- and mesoporous titanosilicate catalysts	0.8, **3.6**	Bimodal narrow PSD at 0.8 and 3.6 nm derived from Ar adsorption at 77 K	[80]
TiO_2 photocatalysts by dissolution of titania-silica binary oxides	Micro[a], **3.9**	Mesoporous photocatalyst with uniform pore size of 4 nm	[81]
Novel preparation of high surface area TiO_2 catalyst	**3.5**, ~10	Variable mesopore size around 10 nm and a fixed contribution at 3.5 nm, suggesting bimodal porosity	[82]
Mesoporous zirconium oxide by sol–gel procedure	**3.6**	Sharp mesopore distribution and high surface area	[83]
Pd/Al_2O_3 by sol–gel preparation	**3.6**, 4.5	Narrow PSD centered at 3.6 nm, finally becoming bimodal at 3.6 and 4.5 nm	[84]
Vanadium phosphorous oxide from vanadyl *n*-butylphosphate	Micro[a], **4.4**	Bimodal distribution with narrow mesopore size at 4.4 nm derived from Dollimore-Heal pore size model	[85]
Preparation of porous SiO_2 from kaolinite	**3.8**	Unimodal pores with average size of 3.8 nm	[86]

[a] The micropore size is not further specified in the manuscript.

Pore network effects

J.C. Groen et al. / Microporous and Mesoporous Materials 60 (2003) 1–17

Acknowledgements

Thanks to Maike Hashagen and Sabine Wrabetz
for measurements and discussion

Thank you for your attention